AJNR

Classification of Biopsy-Confirmed Brain Tumors Using Single-Voxel MR Spectroscopy

M. Elizabeth Meyerand, J. Marc Pipas, Alex Mamourian, Tor D. Tosteson and Jeffery F. Dunn

AJNR Am J Neuroradiol 1999, 20 (1) 117-123
http://www.ajnr.org/content/20/1/117

AJNR Am J Neuroradiol 20:117–123, January 1999

Classification of Biopsy-Confirmed Brain Tumors Using Single-Voxel MR Spectroscopy

M. Elizabeth Meyerand, J. Marc Pipas, Alex Mamourian, Tor D. Tosteson, and Jeffery F. Dunn

BACKGROUND AND PURPOSE: **Our purpose was to develop a classification scheme and method of presentation of in vivo single-voxel proton spectroscopic data from astrocytomas that most closely match the classification scheme determined from biopsy specimens. Since in vivo proton spectroscopy is noninvasive, it may be an attractive alternative to intracranial biopsy.**

METHODS: **Single-voxel spectra were acquired using the point-resolved spectroscopic pulse sequence as part of the Probe spectroscopy package on a G.E. 1.5-T Signa scanner. Subjects consisted of 27 patients with biopsy-confirmed brain tumors (13 with glioblastoma multiforme, six with anaplastic astrocytoma, and eight with low-grade astrocytoma). The patients were divided into groups based on the histologic subtype of their tumor for different treatment protocols.**

RESULTS: **Metabolic peak areas were normalized for each metabolite (choline, creatine, *N*-acetylaspartate, lactate) to the area of the unsuppressed water peak and to the area of the creatine peak. Kruskal-Wallis nonparametric analysis of variance (ANOVA) tests showed statistically significant differences among the tumor groups for all the area ratios. The lactate/water ratio could be used to distinguished all three tumor groups, whereas the choline/water ratio distinguished low-grade astrocytomas from the two high-grade groups. Both the choline and lactate ratios could be used to separate the high-grade from the low-grade tumors.**

CONCLUSION: **Specific relative metabolic peak area ratios acquired from regions of contrast-enhancing brain tumor can be used to classify astrocytomas as to histopathologic grade.**

In vivo MR spectroscopy allows the noninvasive evaluation of metabolic patterns in human brain tumors (1–14). Because of differences in the cell type and growth characteristics of tumors, it is probable that tumor types will have unique metabolic ''fingerprints.'' Our goal was to provide a classification scheme of tumor types that is relative to the treatment program and correlates with biopsy results, but that is totally noninvasive.

The possibility that tumors have unique metabolic fingerprints is supported by a variety of studies. Bruhn et al (6), in a qualitative comparison of in vivo MR spectroscopic findings and histologic data from a variety of brain tumors, showed that histologically similar tumors exhibit similar spectra while histologically different tumors exhibit quite different spectral patterns. Indeed, the relative concentration of these metabolites has been shown to differ depending on whether the tissue is neoplastic or nonneoplastic, rapidly proliferating or slow growing (2, 7, 12). Several studies have shown that a common feature of many rapidly growing tumors is an increased choline to creatine ratio, a decreased *N*-acetylaspartate (NAA) to creatine ratio, and an increased lactate level (1–7, 12, 13). Pruel et al (13) correctly classified 104 of 105 different types of brain tumors by using multivoxel spectroscopy (in which data were analyzed using peak heights).

Our study was designed to differentiate brain tumors by using a combination of single-voxel spectroscopy, biopsy confirmation (which was available from all tumors), and tumor classification (which was related to treatment protocols).

The ability to discriminate among major types of primary brain tumors is critical to effective therapy. The most common types are diffuse, fibrillary astrocytomas (15). These tumors are classified into low-grade astrocytoma (grade I/II), anaplastic astrocytoma (grade III), and glioblastoma multiforme (GBM) (grade IV). There is, however, significant

Received May 1, 1998; accepted after revision August 25.

Supported in part by Norris Cotton Cancer Center core grant 5P30 CA23108–20.

From the Departments of Diagnostic Radiology (M.E.M., A.M., J.F.D.), Community and Family Medicine (T.D.T.), and Hematology and Oncology (J.M.P.), Biomedical NMR Research Lab, Norris Cotton Cancer Center, Dartmouth-Hitchcock Medical Center, Hanover, NH.

Address reprint requests to M. Elizabeth Meyerand, PhD, 8007 Shagbark Circle, Cross Plains, WI 53528.

variation in the clinical course of these lesions and in approach to therapy. Low-grade astrocytoma is a relatively indolent lesion that is treated with surgical resection when possible, often followed by limited-field external-beam radiotherapy. Currently, there is no accepted role for chemotherapy as the primary therapy in this group of patients. Anaplastic astrocytoma is a more aggressive lesion than its low-grade counterpart (15). Survival in this group of patients has been shown to be significantly prolonged by the use of radiotherapy and a three-drug combination chemotherapy regimen known as PCV (CCNU, procarbazine, and vincristine) (16). GBM is an aggressive glial tumor and is the most common primary tumor of the CNS, constituting approximately 20% of all primary neoplasms (15, 17). Most patients with glioblastoma receive radiotherapy. Younger patients with good performance status have been shown to obtain some benefit from the addition of the chemotherapeutic agent bischloronitrosourea (BCNU) (18, 19).

We have designed our experimental protocol such that it can be repeated by any clinical site using FDA-approved single-voxel spectroscopy. In this article we show that these methods provide a high degree of discrimination with respect to treatment-related tumor classification.

Methods

Patients with diagnosed or suspected cerebral neoplasms received MR spectroscopy. The tumors were separated into histologic subtypes that relate to differences in treatment protocol. Those patients with a biopsy-confirmed brain tumor of the types GBM, anaplastic astrocytoma (grade III), and low-grade astrocytoma (I or II) were included in this study (GBM, n = 13; anaplastic, n = 6; low grade, n = 8). If high-grade tumors contained any oligo components, they were classified as mixed neoplasms and were excluded from the study. If a tumor showed any signs of necrosis on histologic examination, the neoplasm was classified as a GBM. Grades I and II tumors were those that did not meet the criteria for anaplastic astrocytomas and did not include pilocytic astrocytomas. Similar spectroscopic examinations were performed in five healthy volunteers. All patients in the study either had never had brain surgery or were at least 2 months beyond surgery (n = 6) at the time of the spectroscopic examination. This allowed us to assume that the enhancing region we included in the MR spectroscopic voxel was most likely living tumor. The patients included 16 women and 11 men with an average age of 43 years (range, 19 to 72 years); the control group included four men and one woman with an average age of 36 years (range, 23 to 44 years).

Water-suppressed, single-voxel spectra were acquired using the point-resolved spectroscopy (PRESS) sequence as part of the Probe spectroscopy package on a G.E. 1.5-T Signa scanner. All spectra were acquired after a contrast-enhanced imaging series so that the viable regions of the tumor would be clearly visible. The size of the voxel was chosen to include as much of the enhancing region of the tumor as possible. The voxel size ranged from 6.2 cm^3 to a minimum voxel size of 1.0 cm^3. Because only enhancing regions of the tumor were included in the voxel volume, the percentage of apparent tumor volume covered by the voxel varied a great deal from tumor to tumor (from approximately 20% to 90%). Tumors smaller than 1.0 cm^3 were not included in the study to avoid partial volume effects from normal tissue. Suspected cystic or necrotic regions were avoided, as were areas near the skull or ventricles. In tumors with an enhancing rim, the voxel size and position were chosen so as to include only the enhancing region. In our study, only the tumors with a histologic classification of GBM showed an enhancing ring and necrotic center on MR images. The PRESS sequence was used with parameters of 2000/272 (TR/TE). These relatively long values were chosen so as to minimize phase-induced baseline distortions and to simplify the resultant spectrum to the four metabolites of interest. One hundred twenty-eight averages were combined for each patient resulting in a scan time of 4 minutes. The standard head coil was used in all cases. The metabolites of interest were lactate at 1.3 ppm, NAA at 2.0 ppm, creatine at 3.0 ppm, and choline at 3.2 ppm.

The spectra were processed on a PC using ProNMR (SoftPulse Software Inc, Ontario, Canada). Line broadening of 3 Hz was followed by Fourier transformation and automatic phase correction. All peaks in the suppressed spectrum were fitted using the Marquardt algorithm subsequent to automated calculation of peak areas. The area data for each peak were expressed relative to that of the unsuppressed water resonance, which was processed in an identical manner (20, 21). T1 saturation and voxel volume differences were not taken into account in this study. Neglecting these parameters may have resulted in small inaccuracies in comparisons among patients.

Results

The data from 27 patients, including spectra and biopsy results, constitute our findings. Examples of spectra from each tumor type and from a healthy control subject are shown in Figure 1.

Ratios of the area of each metabolic peak to the area of the unsuppressed water peak were recorded for each tumor type (Table 1). Kruskal-Wallis nonparametric ANOVA tests showed statistically significant differences among the groups for all the area ratios to water (*P* values listed in Table 1). The strongest group differences were seen for choline and lactate.

Figure 2 shows graphs of area ratios to water for all individual patients. There is no overlap in lactate/water for the three tumor types, indicating that this ratio could be used to differentiate tumor groups. As expected, the high-grade tumors showed a higher relative lactate concentration, with lactate/water ratios between 5.8×10^{-4} and 7.8×10^{-4}. Lactate ratios in control subjects were zero, owing to the undetectable lactate resonance. Figure 2B shows choline/water to be a good index for separating GBMs and anaplastic astrocytomas from low-grade tumors. The choline/water ratios fell in the 5×10^{-4} to 9×10^{-4} range whereas the more slowly growing low-grade tumors had a relatively lower choline concentration.

Ratios with creatine as the internal reference are listed in Table 2. When using creatine as the denominator, both the choline and lactate ratios can be used to separate the high-grade tumors (GBM and anaplastic astrocytomas) from the low-grade tumors (Fig 2C and D). The lactate/creatine ratio (Fig 2D) also differentiated 75% of the grade-III astrocytomas from the GBMs. The low-grade tumors and the control group had lactate/creatine ratios close to zero. In contrast, the high-grade tu-

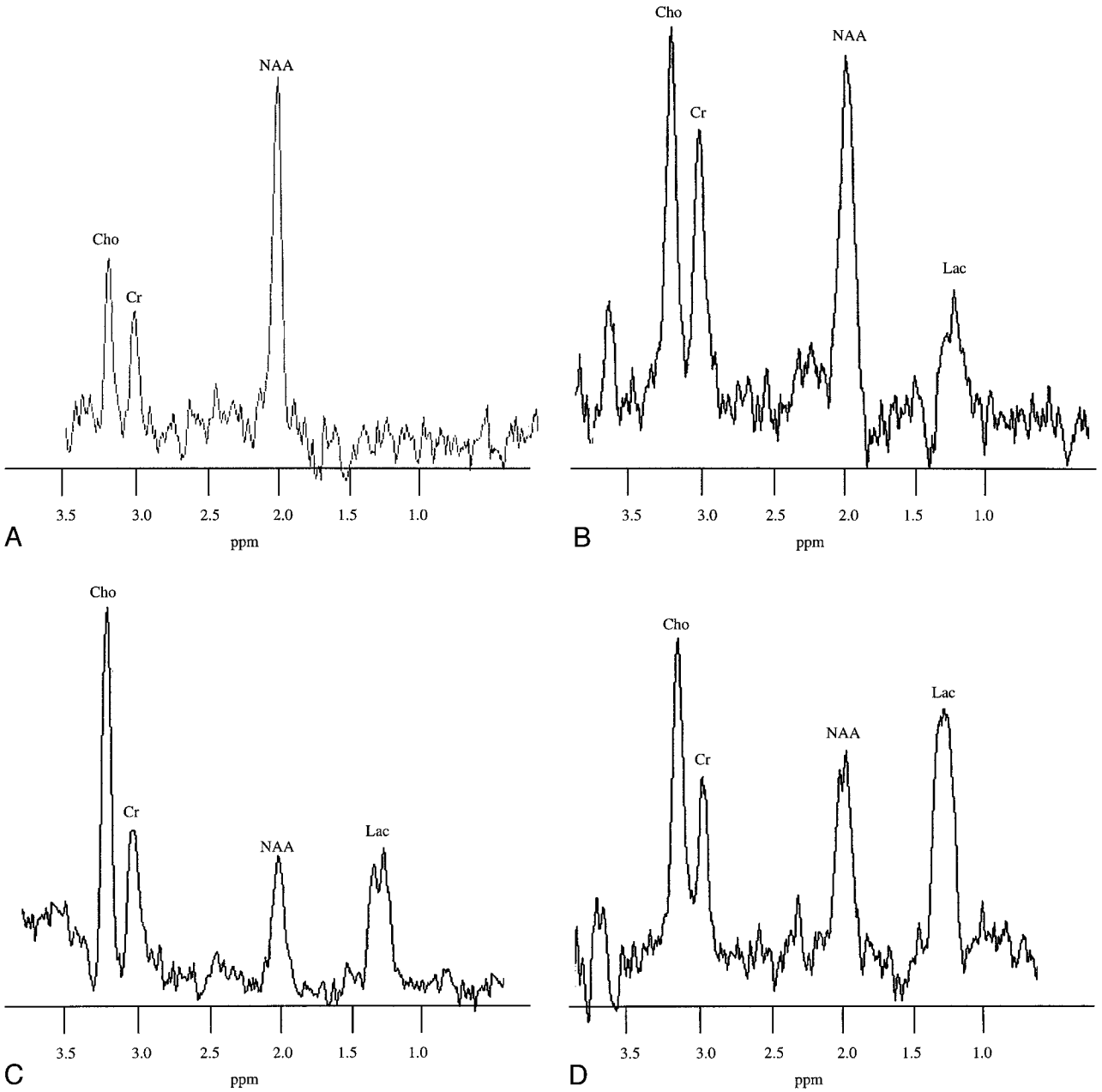

FIG 1. *A–D,* Representative localized in vivo spectra from a healthy control subject (*A*), a 36-year-old patient with a low-grade tumor (*B*), a 21-year-old patient with an anaplastic astrocytoma (*C*), and a 57-year-old patient with a GBM (*D*). In all cases the pulse sequence parameters were 2000/272/128 (TR/TE/excitations).

TABLE 1: The means ± SD intracellular metabolite area ratio to water in the three tumor types and in the control subjects

	Choline (No.)	Creatine (No.)	NAA (No.)	Lactate (No.)
Tumor class				
GBM	0.70 ± 0.10 (13)	0.13 ± 0.02 (13)	0.27 ± 0.05 (13)	0.67 ± 0.05 (13)
Anaplastic	0.73 ± 0.10 (6)	0.13 ± 0.02 (6)	0.17 ± 0.02 (6)	0.41 ± 0.02 (6)
Low-grade	0.13 ± 0.02 (8)	0.16 ± 0.01 (8)	0.26 ± 0.04 (8)	0.01 ± 0.00 (8)
Control subjects	0.15 ± 0.02 (5)	0.18 ± 0.02 (5)	0.39 ± 0.01 (5)	0.00 ± 0.00 (5)
P values	.0001	.002	.0001	.0001

Note.—Numbers in parentheses indicate patients per group. All area ratio values have been multiplied by 1000. GBM indicates glioblastoma multiforme; NAA, *N*-acetylaspartate.

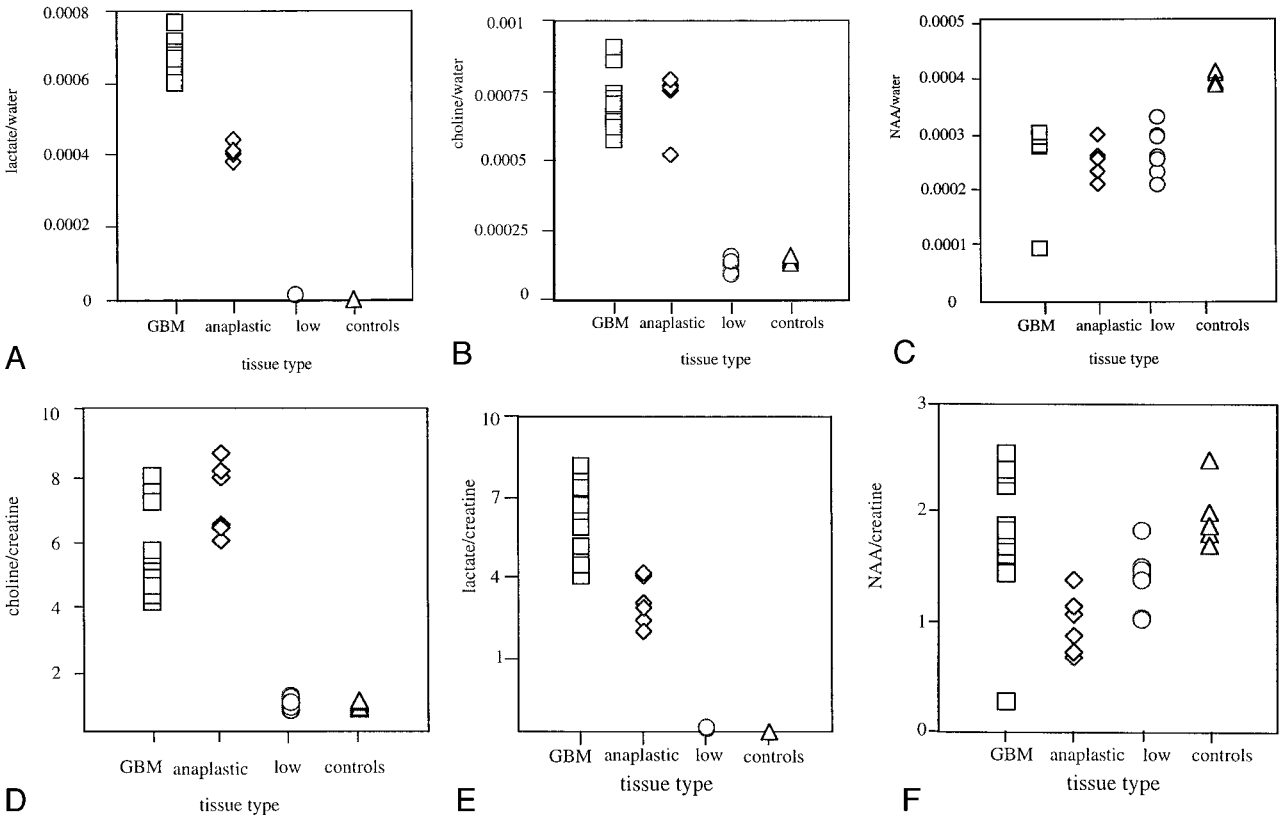

FIG 2. *A–F,* Graphs show the ratios to water and to creatine for the three tumor types in all patients (n = 27) and control subjects (n = 5): lactate to water ratio (*A*), choline to water ratio (*B*), NAA to water ratio (*C*), choline to creatine ratio (*D*), lactate to creatine ratio (*E*), and NAA to creatine ratio (*F*).

TABLE 2: The mean ± SD intracellular metabolite area ratio to creatine in the three tumor types and in the control subjects

	Choline (No.)	NAA (No.)	Lactate (No.)
Tumor Class			
GBM	5.50 ± 1.22 (13)	2.11 ± 0.52 (13)	5.30 ± 0.98 (13)
Anaplastic	7.16 ± 1.10 (6)	1.32 ± 0.23 (6)	3.28 ± 0.59 (6)
Low-grade	0.86 ± 0.17 (8)	1.70 ± 0.25 (8)	0.09 ± 0.01 (8)
Control subjects	0.80 ± 0.11 (5)	2.15 ± 0.25 (5)	0.00 ± 0.00 (5)
P value	.0001	.0015	.0001

Note.—Numbers in parentheses indicate patients per group. GBM indicates glioblastoma multiforme; NAA, *N* -acetylaspartate.

mors had lactate/creatine ratios between 1.3 and 8.0. Although the data set is small, a comparison of results when using water versus creatine as the internal reference indicates that increased discrimination is obtained when using water as the denominator. Dunnett's multiple analysis was performed to determine which ratios differentiate each tumor type from the other two. Results of the test are shown in Tables 3 and 4.

Figure 3 shows simulated average spectra for each group created using SAGE (G.E. Medical Systems, Milwaukee, WI) software. Each spectrum was generated on the basis of Lorentzian lineshapes, using the average peak height and line widths from all individuals in each group. Differences in metabolic concentration between the tumor types appear to be more visually apparent when the data are displayed in this manner. These simulated average spectra also provide the radiologist with typical patterns for comparison of in vivo proton spectra. One can obtain an estimate of the population variability of these peak areas from the standard deviations shown in Table 1.

Discussion

Various investigators have used some form of proton spectroscopy to study tumor metabolism (1–14, 21–23). Our purpose was to focus on the potential of this FDA-approved technique to distinguish among subtypes of cerebral neoplasms. We made no attempt to differentiate tumors from other

TABLE 3: Summary of Dunnett's multiple tests for the data shown in Table 1. The table lists the metabolites (ratio to water) that were statistically significant ($P < .05$) in differentiating each tumor type from the other two. The metabolites are listed at the transections of each tumor type used in the comparison.

	GBM	Anaplastic	Low-Grade	Control Subjects
GBM	···	NAA	Cho, Lac	Cr, Lac
Anaplastic	···	···	Cho	Cho, Cr, NAA
Low-grade	···	···	···	NAA
Control subjects	···	···	···	···

Note.—Cho indicates choline; Lac, lactate, Cr, creatine; NAA, *N*-acetylaspartate; GBM; glioblastoma multiforme.

TABLE 4: Summary of Dunnett's multiple tests for the data shown in Table 2. The table lists the metabolites (ratio to creatine) that were statistically significant ($P < .05$) in differentiating each tumor type from the other two. The metabolites are listed at the transections of each tumor type used in the comparison.

	GBM	Anaplastic	Low-Grade	Control Subjects
GBM	···	NAA	Cho, Lac	Cho, Lac
Anaplastic	···	···	Cho	Cho, NAA
Low-grade	···	···	···	NS
Control subjects	···	···	···	···

Note.—Cho indicates choline; Lac, lactate; Cr, creatine; NAA, *N*-acetylaspartate; GBM, glioblastoma multiforme; NS, statistically not able to differentiate.

nonneoplastic lesions. It has already been shown that in vivo spectroscopy can aid in the differentiation of pathologic processes. Indeed, Rand et al (2) describe an ROC analysis of visual inspection of single-voxel spectra at 0.5 T with a diagnostic accuracy of 0.96 in distinguishing neoplastic from nonneoplastic lesions.

Multivoxel methods can be useful if the goal is to obtain a metabolic map of a large lesion or brain region. Pruel et al (13) were able to correctly classify 104 of 105 tumor spectra. In addition, with the use of multivoxel techniques, voxels containing viable tumor can be identified a priori. However, unless spectral resolution is sacrificed, the acquisition times for multivoxel spectroscopy can be prohibitively long (24).

In single-voxel spectroscopy, the voxel placement is critical to the examination. For this reason, we chose to undertake spectroscopy after a contrast-enhanced MR imaging series had been obtained, as this allows for precise voxel placement over an enhancing region so that signal is acquired only from viable tumor tissue (2, 21, 22).

The optimal pulse sequence parameters for tumor grading are still an issue of debate. Short-TE spectroscopy has the advantage of providing more information, since more peaks are visible for analysis (6). Arguably, this would suggest that short-TE spectra should be used, as the discriminatory power of the metabolic fingerprint should be larger. Conversely, long-TE spectra have less baseline distortion and are easier to quantify (simpler lineshapes and fewer resonances). As a result, data acquired using this technique will have less variability induced by collection and analysis factors. For these reasons we chose long-TE spectroscopy for our study and focused only on the metabolites with longer T2 relaxation times. With the G.E. Probe software, which offers both PRESS and stimulated-echo acquisition mode (STEAM) sequence options, the choice of long-TE values made PRESS the optimum sequence, since there is a $\sqrt{2}$ decrease in the signal-to-noise ratio with STEAM sequences.

Optimum methods for standardization of in vivo proton spectra are also a matter of debate. The method most commonly used is that of taking the ratio of one peak area to another (8, 9, 14). Another approach is to determine carefully the metabolic concentrations in units of mmol/L or weight of brain (25, 26). It is not within the scope of this article to fully discuss the relative merits of the various quantification methods (for reviews, see 27, 28). We chose peak area ratios because of the simplicity of analysis and the previous success of other groups in using the method (8, 9, 14). We also used a ratio to the unsuppressed water resonance, since this is a robust method for standardization. Advantages include minimizing error due to assumptions concerning the experimental setup or operator error (eg, bad voxel delineation, variable field optimization between the sample voxel and a contralateral voxel or an external standard) (21). Also, it is a convenient method to use in conjunction with Probe, since several unsuppressed water spectra are automatically saved along with the water-suppressed spectrum.

Finally, we did not correct for saturation effects, as we were comparing groups of data collected with equal parameters. In addition, it is possible that T1 values change between normal and neoplastic tissues, which would mean that there is no accepted value for correcting saturation. Also, by not correcting for saturation, we may in fact be adding an additional level of discrimination into our area determinations.

Our data show that tumor grades can be differentiated with a high degree of precision using relatively simple, clinically available techniques. There is no overlap between GBMs, high-grade astrocytomas, and low-grade astrocytomas based on the ratio of lactate to water (Fig 2A, Table 1). The ratio of choline to water is also highly correlative with tumor grade (Fig 2B, Table 1), although the capacity to differentiate GBM from high-grade astrocytoma is not as great. The peak ratios to creatine (Table 2) do not have the same discriminatory power, although the numbers in the study group are too small to make a definitive statement at this time.

Our data show that lactate, choline, and NAA have discriminatory power in terms of differentiating tu-

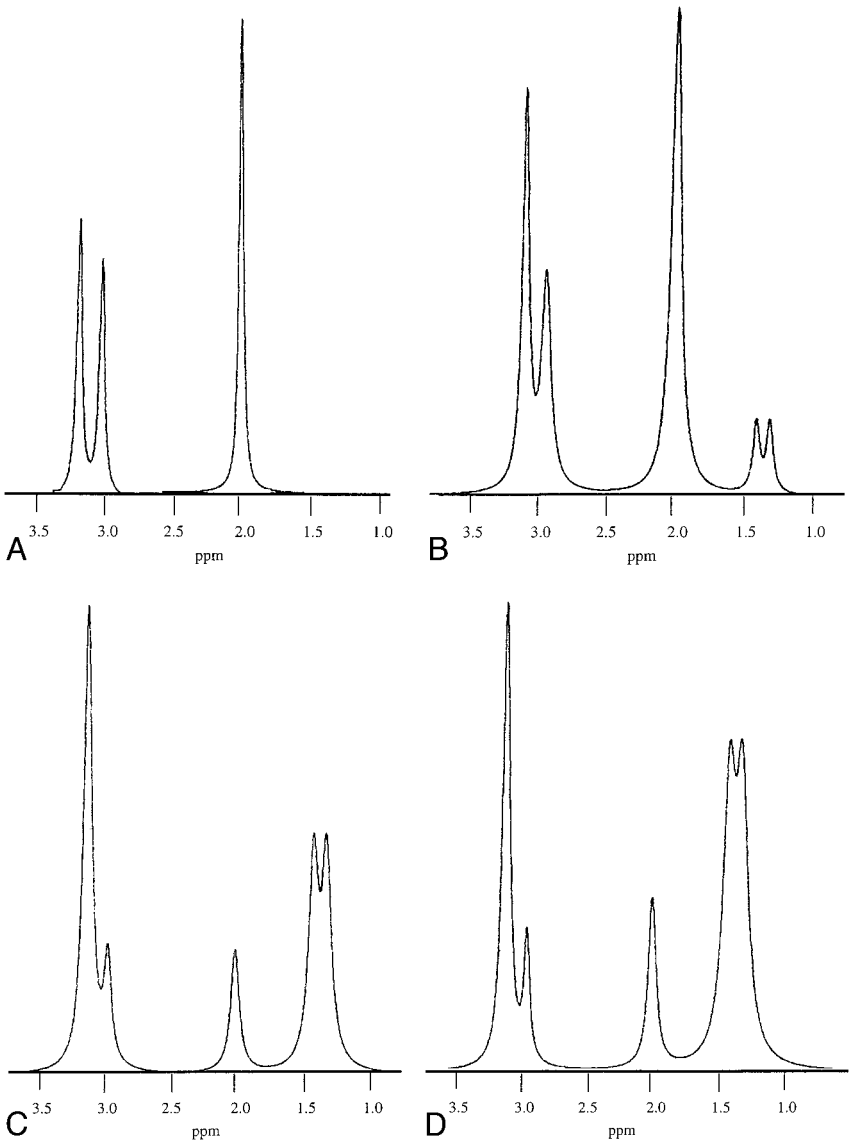

FIG 3. *A–D,* Simulated spectra generated from the average peak heights and linewidths for each patient in all three tumor groups and in the control group. Average spectra from the control subjects (n = 5) (*A*), from the patients with low-grade astrocytomas (n = 8) (*B*), from the patients with anaplastic astrocytomas (n = 6) (*C*), and from the patients with GBMs (n = 13) (*D*).

mor types. The potential for lactate and choline to discriminate among tumors is supported by numerous studies in the past. Using single-voxel spectroscopy and the STEAM pulse sequence with both short (50 msec) and long (270 msec) TEs, Bruhn et al (6) showed an increase in choline in nine primary and secondary tumors. In a study of 122 tumors in 82 patients, Ott et al (9) demonstrated a substantial decrease in NAA/choline for all high-grade tumors using the PRESS sequence and acquisition parameters similar to those used in our study. In addition to an increase in the relative level of choline/creatine, Segebarth et al (8) showed an overall decrease in the level of creatine in a population of 10 patients with glioma by using the STEAM sequence and a long TE. Go et al (14) reported a study in which multivoxel techniques were used in 32 glioma patients, all of whom exhibited an increase in the choline/creatine ratio and a decrease in the NAA/creatine ratio relative to healthy control subjects. In the same study, an increase in lactate/creatine was seen for the malignant gliomas. Tedeschi et al (1) used choline as an indicator of the progression of neoplasms and showed that over a 3-1/2–year period, all progressive tumors had an increase in the choline concentration of over 45%, whereas all stable tumors showed a 35% increase or less. These results support our findings that choline and lactate are accurate markers for differentiating among tumor grades.

Several studies have postulated that elevated choline may reflect an increase in the concentration of the spectroscopically detectable metabolites that are precursors of membrane phospholipids needed to support the increased cell turnover in neoplastic tissue (8, 27, 29). A decreased NAA/creatine ratio is consistent with the replacement of healthy neurons by neoplastic cells (14). Lactate, an end-product of anaerobic glycolysis, is often elevated in rapidly growing tumors, in which hypoxic regions may exist (8, 27, 29).

Conclusion

We have shown that specific metabolites, when standardized to water, are of diagnostic value in the division of tumors into three categories. Specifically, the lactate/water ratio can be used to differentiate GBMs, anaplastic astrocytomas, and low-grade tumors, as there is no overlap in the relative area ratios among these three groups. The choline/water, choline/creatine, and lactate/creatine ratios can be used to distinguish high-grade from low-grade tumors, as there is no overlap between these two groups of data. The results of this study also suggest that quantitation in terms of obtaining the absolute concentration of each metabolite is not required to differentiate among tumor types. Tumor types were differentiated solely on the basis of relative differences normalized to water. It is hoped that this technique will give physicians treating patients with primary brain tumors additional information in diagnosing and monitoring these diseases.

Acknowledgments

We thank Robert W. Prost for his assistance in creating the simulated spectra and Julia Weiss for her assistance in statistical programming.

References

1. Tedeschi G, Lundbom N, Raman R, et al. **Increased choline signal coinciding with malignant degeneration of cerebral gliomas: a serial proton magnetic resonance spectroscopy imaging study.** *J Neurosurg* 1997;87:516–524
2. Rand SD, Prost R, Haughton V, et al. **Accuracy of single-voxel proton MR spectroscopy in distinguishing neoplastic from non-neoplastic brain lesions.** *AJNR Am J Neuroradiol* 1997;18: 1695–1704
3. Demaerel P, Johannik K, Van Heche P, et al. **Localized H-1 NMR spectroscopy in fifty cases of newly diagnosed intracranial tumors.** *J Comput Assist Tomogr* 1991;15:67–76
4. Miller BL, McBride D, Riedy G, Caron M, Lipcamon J, O'Brien D. **Changes in brain choline in tumors with H-1 NMR spectroscopy.** *Bull Clin Neurosci* 1990;55:115–122
5. Sijens PE, Knopp MV, Brunetti A, et al. **H-1 spectroscopy in patients with metastatic brain tumors: a multicenter study.** *Magn Reson Med* 1995;33:818–826
6. Bruhn H, Frahm J, Gyngell ML, et al. **Noninvasive differentiation of tumors with use of localized H-1 MR spectroscopy in vivo: initial experience in patients with cerebral tumors.** *Radiology* 1989;172:541–548
7. Poptani H, Gupta RK, Roy R, Pandey R, Jain VK, Chhabra DK. **Characterization of intracranial mass lesions with in vivo proton MR spectroscopy.** *AJNR Am J Neuroradiol* 1995;16: 1593–1603
8. Segebarth CM, Baleriaux DF, Luyten PR, den Hollander JA. **Detection of metabolic heterogeneity of human intracranial tumors in vivo by H-1 NMR spectroscopic imaging.** *Magn Reson Med* 1990;13:62–76
9. Ott D, Hennig J, Ernst T. **Human brain tumors: assessment with in vivo proton MR spectroscopy.** *Radiology* 1993;186:745–752
10. Fulham MJ, Bizzi A, Diatz MJ, et al. **Mapping of brain tumor metabolites with proton MR spectroscopic imaging: clinical relevance.** *Radiology* 1992;185:675–686
11. Yamagata NT, Miller BL, McBride D, et al. **In vivo proton spectroscopy of intracranial infections and neoplasms.** *J Neuroimaging* 1994;4:23–28
12. Negendank WG, Sauter R, Brown TR, et al. **Proton magnetic resonance spectroscopy in patients with glial tumors: a multicenter study.** *J Neurosurg* 1996;84:449–458
13. Pruel MC. **Accurate noninvasive diagnosis of human brain tumors by using proton magnetic resonance spectroscopy.** *Nature Med* 1996;2:323–325
14. Go KG, Kamman RL, Mooyaart EL, et al. **Localized proton spectroscopy and spectroscopic imaging in cerebral gliomas, with comparison to positron emission tomography.** *Neuroradiology* 1995;37:198–206
15. Devita VT, Hellman S, Rosenberg SA, et al. *Cancer: Principles and Practice of Oncology.* 5th ed. Philadelphia: Lippincott-Raven; 1997:2013–2015
16. Levin VA, Silver P, Hannigan J, et al. **Superiority of post-radiotherapy adjuvant chemotherapy with CCNU, procarbazine, and vincristine (PCV) over BCNU for anaplastic gliomas: NCOG6G61 final report.** *Int J Radiat Oncol Biol Phys* 1990;18: 321–324
17. Damjanov I, Linder J, eds. *Anderson's Pathology.* 9th ed. St Louis: Mosby; 1990:2168
18. Devita VT, Hellman S, Rosenberg SA, et al. *Cancer: Principles and Practice of Oncology.* 5th ed. Philadelphia: Lippincott-Raven; 1997:2043–2047
19. Fine HA, Dear KBG, Loeffler JS, Black PM, Canellos GP. **Meta-analysis of radiation therapy with and without adjuvant chemotherapy for malignant gliomas in adults.** *Cancer* 1993;71: 2585–2597
20. Somorjai RL, Dolenko B, Nikulin AK, et al. **Classification of 1H MR spectra of human brain neoplasms: the influence of preprocessing and computerized consensus diagnosis on classification accuracy.** *J Magn Reson Imaging* 1996;6:437–444
21. Soher BJ, Hurd RE, Sailasuta N, Barker PB. **Quantitation of automated single-voxel proton MRS using cerebral water as an internal reference.** *Magn Reson Med* 1996;36:335–339
22. Houkin K, Kamada K, Sawamura Y, et al. **Proton magnetic resonance spectroscopy (1H-MRS for the evaluation of treatment of brain tumors.** *Neuroradiology* 1995;37:99–103
23. Chang L, McBride D, Jenden D, et al. **Localized in vivo 1H magnetic resonance spectroscopy and in vitro analyses of heterogeneous brain tumors.** *J Neuroimaging* 1995;5:157–163
24. Posse S, Dager RS, Richards TL, et al. **In vivo measurement of regional brain metabolic response to hyperventilation using magnetic resonance: proton echo planar spectroscopic imaging (PEPSI).** *Magn Reson Med* 1997;37:858–865
25. Kreis R, Ernst T, Ross BD. **Development of the human brain: in vivo quantification of metabolite and water content with proton magnetic resonance spectroscopy.** *Magn Reson Med* 1993;30:1–14
26. Bovee WMMJ. **Quantification of glutamate, glutamine, and other metabolites in in vivo proton NMR spectroscopy.** *NMR Biomed* 1991;4:81–84
27. Ross BD, Michaelis T. **Clinical applications of magnetic resonance spectroscopy.** *Magn Reson Q* 1994;10:191–247
28. Bottomley PA. **Human in vivo NMR spectroscopy in diagnostic medicine: clinical tool or research probe?** *Radiology* 1989;170: 1–15
29. Negandank WG, Sauter R, Brown TR, et al. **Proton magnetic resonance spectroscopy in patients with glial tumors: a multicenter study.** *J Neurosurg* 1996;84:449–458